# Sea surface $p$CO$_2$ cycles and CO$_2$ fluxes at landfast sea ice edges in Amundsen Gulf, Canada

B. G. T. Else,[1] R. J. Galley,[1] T. N. Papakyriakou,[1] L. A. Miller,[2] A. Mucci,[3] and D. Barber[1]

[1]  In late fall, spring, and early summer, we measured the surface ocean and atmospheric partial pressures of CO$_2$ ($p$CO$_{2sw}$ and $p$CO$_{2atm}$, respectively) to calculate CO$_2$ gradients ($\Delta p$CO$_2$ = $p$CO$_{2sw}$ − $p$CO$_{2atm}$) and resulting fluxes along the landfast ice regions of southern Amundsen Gulf, Canada. In both the fall and spring seasons we observed positive $\Delta p$CO$_2$ caused by wind-driven upwelling. The presence of a landfast ice edge appeared to be an important factor in promoting this upwelling in some instances. Despite the potential for significant CO$_2$ evasion, we calculated small fluxes during these periods due to high sea ice concentration. In summer, $\Delta p$CO$_2$ became strongly negative across the entire study area. Primary production no doubt played a role in the $p$CO$_{2sw}$ drawdown, but we found evidence that sea ice melt and dissolution of ice-bound calcium carbonate crystals may also have been contributing factors. The seasonal $\Delta p$CO$_2$ cycle suggests a net annual sink of atmospheric CO$_2$ for these landfast ice regions, since calculated summer uptake by the ocean was much stronger than fall/spring outgassing and occurred over a longer time period. However, we hypothesize that this balance is highly dependent on the strength of upwelling and the timing of ice formation and decay, and therefore may be influenced by interannual variability and the effects of climate change.

## 1. Introduction

[2]  Landfast sea ice is essentially motionless ice that is either anchored to the coast or seabed, or is constrained by narrow channels. Unlike a mobile ice cover, which is typically composed of some fraction of open water, landfast ice is usually characterized by a complete ice coverage (i.e., ice concentration of 10/10$^{ths}$ [*Galley et al.*, 2012]). Cracks may occur due to tidal heaving (particularly near the coast), and the ice may decay to the point where thaw holes melt through the ice in late summer [*Jacobs et al.*, 1975], but for most of its temporal and spatial extent landfast ice acts as a separation between ocean and atmosphere.

[3]  Across this separation, significant air-sea gradients of CO$_2$ (defined as $\Delta p$CO$_2$ = $p$CO$_{2sw}$ − $p$CO$_{2atm}$, where *sw* and *atm* denote the partial pressure of CO$_2$ in the surface seawater and atmosphere, respectively) can develop. In Prydz Bay, Antarctica, *Gibson and Trull* [1999] observed strongly negative $\Delta p$CO$_2$ under landfast ice in the spring and fall, and a gradual increase in $p$CO$_{2sw}$ over the winter that approached equilibrium with the atmosphere (i.e. $\Delta p$CO$_2$ = 0). *Fransson et al.* [2009] reported strongly negative $\Delta p$CO$_2$ associated with summer landfast ice in the Canadian Arctic Archipelago, while *Sejr et al.* [2011] found persistent negative gradients under the landfast ice of a fjord in northeastern Greenland.

[4]  The development of under-ice CO$_2$ gradients are a result of biogeochemical and physical processes that are heavily influenced by the sea ice itself. During the winter, low incoming solar radiation is further attenuated by sea ice and the overlying snowpack, limiting photosynthesis. Under these conditions, respiration is expected to dominate over photosynthesis, explaining in part observed under-ice increases of $p$CO$_{2sw}$ in the winter [*Gibson and Trull*, 1999; *Miller et al.*, 2002; *Else et al.*, 2012; *Shadwick et al.*, 2011]. Part of the increase can also be explained by the addition to the mixed layer of brines, which typically have high $p$CO$_{2sw}$ in winter due to impurity rejection during ice formation and the retention of alkalinity by calcium carbonate crystals within the ice volume [*Rysgaard et al.*, 2007; *Dieckmann et al.*, 2008]. With the advent of spring, sufficient light penetrates to the base of the sea ice to maintain ice algae communities that draw down $p$CO$_{2sw}$ [*Gibson and Trull*, 1999; *Else et al.*, 2012; *Shadwick et al.*, 2011], and ice melt further lowers $p$CO$_{2sw}$ by dilution

---

[1]Centre for Earth Observation Science, Department of Environment and Geography, University of Manitoba, Winnipeg, Manitoba, Canada.

[2]Institute of Ocean Sciences, Fisheries and Oceans Canada, Sidney, British Columbia, Canada.

[3]GEOTOP, Department of Earth and Planetary Science, McGill University, Montreal, Quebec, Canada.

Corresponding author: B. G. T. Else, Centre for Earth Observation Science, Department of Environment and Geography, University of Manitoba, Wallace Building, 125 Dysart Rd., Winnipeg, MB R3T 2N2, Canada. (b_else@umanitoba.ca)
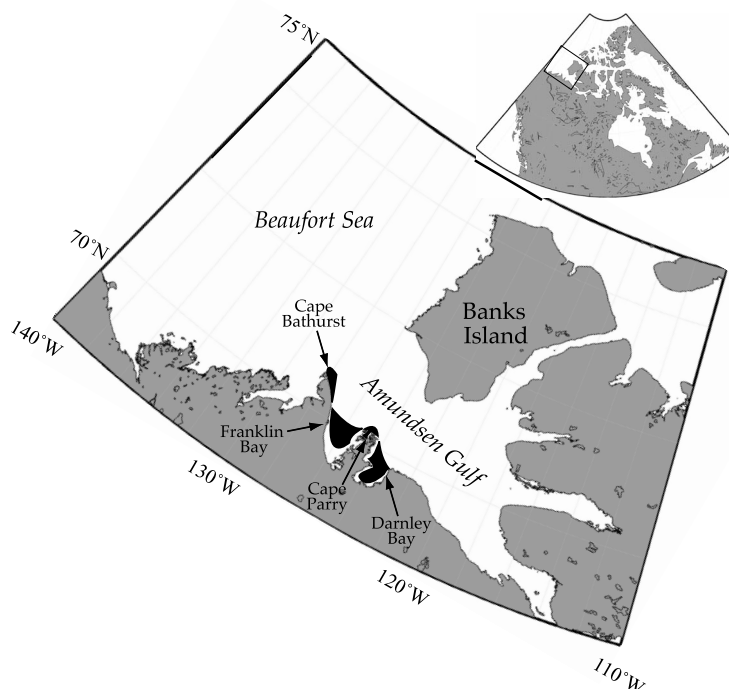
**Figure 1.** Map of the study area. Black polygons/points indicate areas where landfast ice sampling occurred.

and the dissolution of calcium carbonate crystals [*Rysgaard et al.*, 2007, 2009]. Eventually, the ice cover is removed and spring open water phytoplankton blooms (potentially seeded by ice algae) may further lower $pCO_{2sw}$.

[5] These processes should precondition landfast ice areas to absorb atmospheric $CO_2$ once the ice cover is removed [e.g., *Gibson and Trull*, 1999], but there is some debate about whether or not air-sea $CO_2$ exchange can occur across the sea ice boundary. If gases can travel through sea ice, then winter air-sea gas exchange (including possible outgassing of $CO_2$) could occur in landfast ice regions. Both *Gosink et al.* [1976] and *Loose et al.* [2011] have shown that gases can diffuse through sea ice, but their observed exchange rates were several orders of magnitude lower than even the most modest exchange through open water. Accordingly, *Loose et al.* [2011] proposed that transfer through leads and other open water portions of the icescape is the dominant pathway for air-sea gas exchange in seasonal ice environments.

[6] In this paper, we focus on understanding the air-sea exchange of $CO_2$ in the landfast ice regions of Amundsen Gulf, Canada. We adopt the *Loose et al.* [2011] hypothesis that no significant gas exchange occurs across the sea ice boundary, and assume that the net air-sea exchange of $CO_2$ is determined during the ice-free or partially ice-free seasons. Exchanges of $CO_2$ between the solid ice surface and the atmosphere – which may be important in some seasons [e.g., *Papakyriakou and Miller*, 2011; *Nomura et al.*, 2010; *Semiletov et al.*, 2004] – are not considered in this study, but have been investigated by others [*Miller et al.*, 2011; *Geilfus et al.*, 2012]. Hence, the objectives of this work are: (1) to examine how the landfast ice interacts with biogeochemical cycles to generate $pCO_{2sw}$ gradients, and (2) to estimate the

air-sea exchange of $CO_2$ arising from those gradients, focusing on the role of sea ice in modulating gas exchange.

## 2. Methods

### 2.1. Study Area

[7] This study was conducted in the landfast ice surrounding Amundsen Gulf, a relatively deep coastal channel connecting the Canadian Arctic Archipelago (CAA) to the southeastern Beaufort Sea (Figure 1). Sea ice in the middle of Amundsen Gulf is usually mobile throughout the winter, while ice on the periphery becomes landfast as early as the first week of November [*Galley et al.*, 2012]. The region is best known to the scientific community as the site of the Cape Bathurst polynya, which typically forms in the first week of June with the dynamic export of sea ice out of Amundsen Gulf [*Galley et al.*, 2008]. Ice on the periphery, however, typically remains landfast until early July [*Galley et al.*, 2012] before a combination of dynamic and thermodynamic forcings removes the ice cover.

[8] During the 2007–08 International Polar Year, the research icebreaker CCGS *Amundsen* spent nearly 10 months in this area conducting ArcticNet projects [*ArcticNet Inc.*, 2010] and the Circumpolar Flaw Lead System Study [*Barber et al.*, 2010]. On several occasions, the research vessel sailed into the landfast ice along the southern margin of Amundsen Gulf. Fast ice sites in Franklin Bay, Darnley Bay, Cape Bathurst and Cape Parry (Figure 1) were visited in early November 2007, and then studied extensively in June 2008 as the ice edges decayed.

## 2.2. Sampling

[9] To measure $pCO_{2sw}$ we used a custom-built equilibrator, which sampled at one minute intervals. The system was composed of a cylindrical tank with a shower inlet supplied by water diverted from a high-volume scientific intake at ~5 m depth. Headspace air in the tank was cycled through a desiccant column and an LI-7000 gas analyzer that measured the dry air mixing ratio of $CO_2$ ($xCO_2$). A continuous stream of ultra-high purity $N_2$ was passed through the reference cell of the LI-7000 to reduce sensor drift, and the instrument was calibrated daily using a certified gas standard with a concentration of 379.4 ppm. The mean rate of sensor drift during the experiment was 0.03 ppm hr$^{-1}$, resulting in calibration-to-calibration drift that was typically on the order of 0.7 ppm. We calculated $pCO_{2sw}$ from $xCO_2$ as follows:

$$pCO_{2sw} = xCO_2 \times (P - pH_2O) \qquad (1)$$

where $P$ is the atmospheric pressure, and $pH_2O$ is the saturation vapor pressure of air in the equilibration chamber (determined empirically from water temperature and salinity using the equations of *Weiss and Price* [1980]). Although the intake was fairly close (~5 m) to the equilibrator, a correction was required to account for warming of the seawater relative to *in situ* conditions [*Takahashi et al.*, 1993]. The warming was typically on the order of ~1.5°C, and after correction the system showed good correspondence with independent estimates of $pCO_{2sw}$ obtained from bottle cast measurements of carbonate system chemistry (see *Else et al.* [2011, 2012] for further details).

[10] A comparison of the $pCO_{2sw}$ sensor output with measurements from a thermosalinograph sampling the same inlet streams showed a lag time in the equilibrator on the order of 5–10 minutes. For stationary applications this was not a significant problem, but when the ship was moving we offset the $pCO_{2sw}$ sample times by 7 minutes to allow better synchronicity between the two instruments. The thermosalinograph sensor also sampled at one-minute intervals, and was used as the primary data source for sea surface salinity and temperature used in equation (1), and for the interpretation of $pCO_{2sw}$ data. When the thermosalinograph data were unavailable (due to sensor malfunction), we used data from CTD casts when sampling on station.

[11] Atmospheric $CO_2$ measurements were obtained with a separate LI-7000 connected to a gas sampling system that drew air from an inlet located on a bow-mounted meteorological tower, ~14 m above the water surface. A continuous $N_2$ stream was passed through the reference cell, and the system was calibrated daily with a certified standard (two standards were used throughout the year-long study, with concentrations of 381.5 and 383.7 ppm), achieving a mean drift <0.01 ppm hr$^{-1}$. Mixing ratio measurements were converted to $pCO_{2atm}$ (at saturated water vapor pressure) using a similar approach to equation (1), and data were filtered based on wind direction (measurements where wind direction was ±30° of directly astern were discarded) to remove instances where the gas analyzer might have been contaminated by emissions from the ship's smokestack [*Else et al.*, 2011].

## 2.3. CO$_2$ Flux Calculations

[12] For ice-affected seas, air-sea $CO_2$ flux ($F_{CO_2}$) is commonly estimated using a standard form of the bulk flux equation, scaled by the ice concentration ($C_i$, measured in tenths):

$$F_{CO_2} = k\alpha(pCO_{2sw} - pCO_{2atm})(1 - C_i/10) \qquad (2)$$

where $k$ is the gas transfer velocity, $\alpha$ is the solubility of $CO_2$ in seawater and $pCO_{2atm}$ is the partial pressure of $CO_2$ in the overlying atmosphere. This approach is fundamentally sound (assuming that sea ice does not act as a conduit for air-sea exchange), but only if the choice of $k$ parameterization is appropriate. When $C_i$ is greater than 0 (but less than 10), the open water patches are fetch-limited, which is expected to reduce $k$ relative to open water conditions [e.g., *Woolf*, 2005]. Unfortunately, useful parameterizations that account for this effect do not exist, forcing the use of parameterizations developed for ice free oceans. Although this approach is now common, we stress that it should be used with the understanding that $F_{CO_2}$ will likely be overestimated to some degree. In this study, we used the $k$ parameterization of *Sweeney et al.* [2007]:

$$k = 0.27U^2(Sc/660)^{(-1/2)} \qquad (3)$$

where $Sc$ is the Schmidt number (a function of sea surface temperature (SST) as per *Jähne et al.* [1987]), and $U$ is the wind velocity at 10 m height.

[13] We used this approach to estimate air-sea $CO_2$ flux in our study area during ice formation, breakup, and the open water season. When a location became landfast ($C_i = 10$), we assumed that the air-sea flux was negligible [*Loose et al.*, 2011]. The calculations were made using the one-minute measurements of $pCO_{2sw}$ and $pCO_{2atm}$ for the periods during which the research vessel was in the vicinity of Franklin Bay, Darnley Bay, Cape Parry and Cape Bathurst (Figure 1). Ice concentration was obtained from digital ice charts prepared by the Canadian Ice Service (CIS), which were typically available every 2–5 days during our study. For wind velocity, we used one-minute sampling interval data recorded on the ship's meteorological tower at a height of ~14 m, scaled to a height of 10 m assuming a logarithmic wind profile (see *Else et al.* [2011] for instrument details and quality control information).

[14] Since the research vessel was not always in the study area, we also used wind velocity measurements from the Cape Parry Environment Canada station (Figure 1) to help understand seasonal wind conditions in the area. This station is located at ~90 m above sea level on a small spit of land which extends into Amundsen Gulf. When wind velocities are scaled to 10 m height, they are in reasonable agreement with ship-based velocities and directions (mean differences in x/y wind components <3 m s$^{-1}$).

## 3. Results

### 3.1. $pCO_{2sw}$ and Landfast Ice Cycles

#### 3.1.1. Fall/Winter (October–November 2007)

[15] Observations made at the landfast ice sites in autumn 2007 are summarized in Figure 2. In late October (Figure 2a), Franklin and Darnley Bays were not yet covered by landfast ice, but were mostly covered by newly forming ice. At that time, $pCO_{2sw}$ was fairly low (mean 320 $\mu$atm, standard deviation ±13 $\mu$atm) in offshore Amundsen Gulf [see also

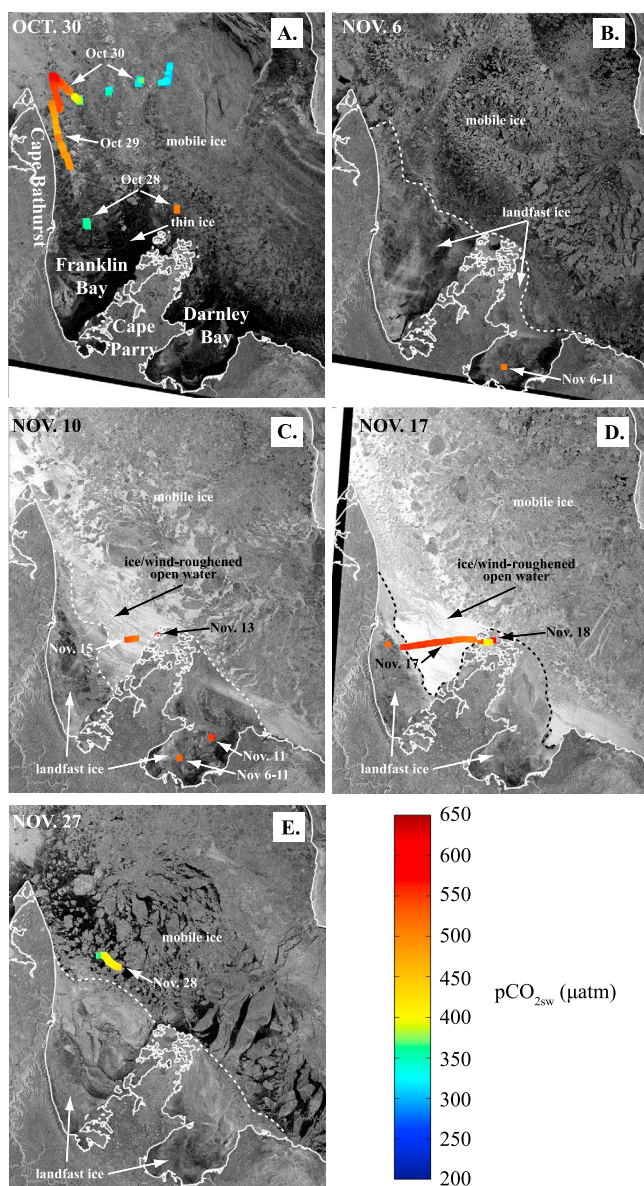**Figure 2.** Measured $pCO_{2sw}$ ($\mu$atm) during transects conducted in October–November 2007. Transects are overlain on RADARSAT-1 SAR imagery, with the image dates noted in the top left corner. The dashed lines (white or black) denote the landfast ice edges, as identified by the Canadian Ice Service (CIS). Additional annotations are included to help with interpretation of ice features from the SAR imagery. The images are RADARSAT-1 ScanSAR wide with 50 m pixel spacing, obtained from RADARSAT International. Images were calibrated to $\sigma^o$ and projected on the CIS Lambert Conformal Conic projection.

*Else et al.*, 2012], but was much higher in the landfast ice forming areas (Figure 2a); $pCO_{2sw}$ was $363 \pm 9$ $\mu$atm in Franklin Bay, $493 \pm 25$ $\mu$atm near Cape Bathurst and $508 \pm 4$ $\mu$atm near Cape Parry.

[16] The elevated coastal $pCO_{2sw}$ relative to the offshore measurements can be linked to fall upwelling events [*Tremblay et al.*, 2011; *Else et al.*, 2012]. The vertical distribution of water

masses in this area is fairly typical for the Arctic Ocean [*Shadwick et al.*, 2011]; a relatively fresh polar mixed layer (PML) overlies a steep halocline that is characterized by salinity in the range of 32–35. Between October 8–20, three storms occurred with sustained easterly (along-shore) winds in excess of 15 m s$^{-1}$ (Figure 3a) that provided the necessary conditions for upwelling of saline halocline waters to the surface. In late October, surface salinity in offshore Amundsen Gulf ranged from 28.0 to 29.6, while salinity near the coast ranged from 31.5 to 33.2. Salinity was particularly high ($\sim$32.7) along Cape Bathurst, an area known for bathymetry-induced upwelling [*Williams and Carmack*, 2008], and Cape Parry (31.7), an area with similar bathymetric features. Since $pCO_{2sw}$ in Amundsen Gulf increases rapidly with depth [*Shadwick et al.*, 2011; *Lansard et al.*, 2012], this upwelling brought with it $CO_2$-rich water to the surface, contributing to the high near-shore $pCO_{2sw}$ reported in Figure 2a.

[17] Measurements made about two weeks later (Figures 2b and 2c) show that similar upwelling also occurred in Darnley Bay. According to CIS charts and ship-based observations, the ice in Darnley Bay was landfast by November 6 (Figure 2b) when the CCGS *Amundsen* entered the Bay. A station in the southern half of the Bay was occupied until November 11, where we measured $pCO_{2sw}$ of $530 \pm 14$ $\mu$atm and salinity of 33.2. From there, the ship traveled to a small bay near Cape Parry (Figure 2c), where $pCO_{2sw}$ had increased by approximately 100 $\mu$atm (to $598 \pm 5$ $\mu$atm) since the previous measurement in the area (Figure 2a), suggesting that upwelling intensified as the season progressed (unfortunately no salinity samples were available at that station). The intensifying upwelling was no doubt driven by strong easterly winds that persisted throughout early November (Figure 3a), and was eventually responsible for the very high $pCO_{2sw}$ (500–560 $\mu$atm, Figure 2d) and salinity (33.2) in Franklin Bay measured between November 16–18 (Figures 2b and 2c).

[18] The timing of fall landfast ice formation varied throughout the study area. The first ice charts to show landfast ice in Franklin and Darnley Bays were dated November 6 (Figure 2b), although subsequent strong winds mobilized the ice in the northern portion of the Bays (Figures 2c and 2d). After winds died down around November 18, the landfast ice in the bays re-established itself (Figure 2e) and persisted throughout most of the winter. The ice around Cape Parry became landfast at around the same time, while the Cape Bathurst region did not become landfast until January. At its maximum extent, landfast ice stretched across the mouth of Franklin Bay from Cape Bathurst to Cape Parry, and across the mouth of Darnley Bay from Cape Parry eastwards.

### 3.1.2. Early Spring (May 2008)

[19] This maximum landfast ice extent was not sustained throughout the winter; CIS charts show the landfast edge migrating southwards as early as February 17 in Franklin Bay, eventually culminating in a significant fracture of the northern quarter of the landfast ice around April 15. This fracture allowed the CCGS *Amundsen* to travel along the margin between the new landfast ice edge and the fractured ice in early May (Figure 4). As Figure 4a shows, $pCO_{2sw}$ was still high (430–500 $\mu$atm) in Franklin Bay, and near Cape Parry ($531 \pm 16$ $\mu$atm) in mid-May.

[20] Lacking a complete time series, it is difficult to know how $pCO_{2sw}$ was modified through the winter to produce the levels that we observed in May (Figure 4a). In
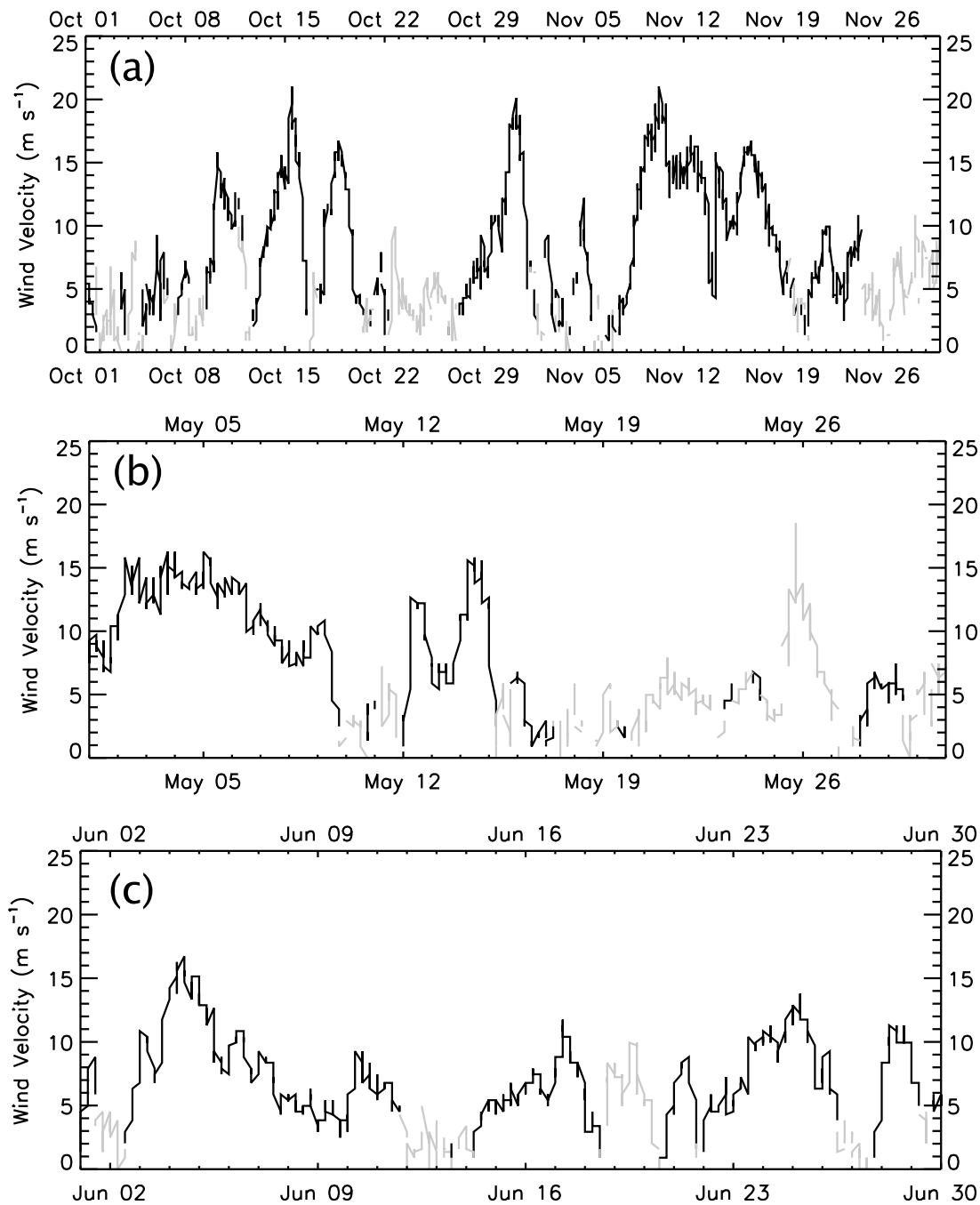
**Figure 3.** Wind velocity measurements from the Cape Parry weather station for the three time periods discussed in the text. The dark black lines indicate winds from an upwelling-favorable (easterly) direction.

both Franklin Bay and Cape Parry, $p$CO$_{2sw}$ decreased by ~60–70 $\mu$atm relative to November 2007 measurements, and surface salinity decreased to 32.9 (from 33.2 in Franklin Bay). The decreased salinity indicates that advective mixing must have taken place (melt is unlikely given that air temperatures were still consistently below $-10°$C), replacing to some extent the PML water that was displaced by the fall upwelling. Without such mixing we would have expected salinity to increase over the winter due to brine rejection as was observed in Amundsen Gulf [*Shadwick et al.*, 2011], and in Franklin

Bay during the 2003–04 winter [*Miller et al.*, 2011]. The lower $p$CO$_{2sw}$ (maximum 382 $\mu$atm [*Else et al.*, 2012]) and fresher (maximum salinity ~31.5 [*Shadwick et al.*, 2011]) surface waters of Amundsen Gulf are the likely source water for this mixing. Under-ice biological activity may also have played a role in lowering $p$CO$_{2sw}$; in Amundsen Gulf we estimated a biological reduction in $p$CO$_{2sw}$ on the order of ~15 $\mu$atm between March and early May [*Else et al.*, 2012], and the ice algae biomass was 4–8 times higher under the landfast ice in Franklin Bay [*Tremblay et al.*, 2011].
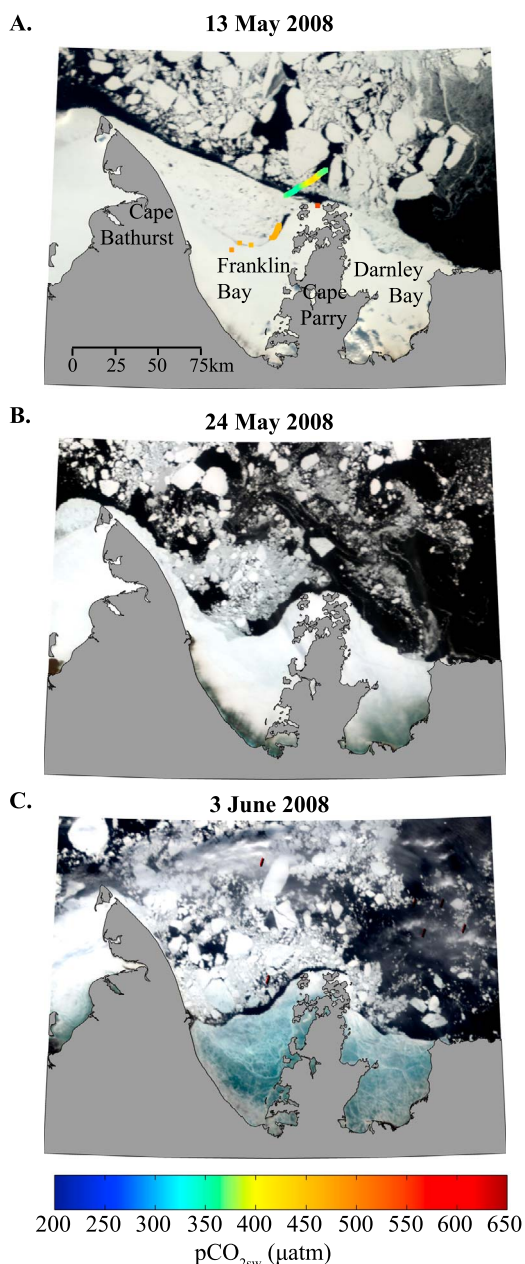
**A.** 13 May 2008

Cape Bathurst

Franklin Bay

Cape Parry

Darnley Bay

0   25   50   75km

**B.** 24 May 2008

**C.** 3 June 2008

200  250  300  350  400  450  500  550  600  650

$pCO_{2sw}$ ($\mu$atm)

**Figure 4.** Measured $pCO_{2sw}$ ($\mu$atm) during transects conducted in May 2008. Transects are overlain on true-color MODIS imagery. Note that no $pCO_{2sw}$ are plotted in Figures 4b and 4c – they have been included to show the evolution of the landfast ice during the month of May.

### 3.1.3. Late Spring/Summer (June 2008)

[21] The ship's initial return to the area in June corresponded with the final departure of ice from the northern quarter of Franklin Bay (compare Figures 4c, 5a and 5b). Patches of very low (250–275 $\mu$atm) $pCO_{2sw}$ were observed just seaward of the Darnley Bay ice edge (Figure 5a), and a mean $pCO_{2sw}$ of 293 ± 11 $\mu$atm was observed approximately 1 km into the ice. Assuming that conditions in May were similar to Cape Parry and Franklin Bay, $pCO_{2sw}$ decreased by ~200 $\mu$atm and salinity by ~1.8 over 4 weeks

in the region. We estimate the ice melt contribution to $pCO_{2sw}$ decrease to be ~16 $\mu$atm per unit of salinity, assuming conservative mixing between measurements of the carbonate system in meltwater [*Lansard et al.*, 2012] and the PML for this region in June [*Shadwick et al.*, 2011]. Therefore, ice melt was responsible for only ~30 $\mu$atm of the decrease from early May. Sea surface temperature remained near the freezing point during this time period and stratification due to ice melt would have limited vertical mixing, leaving biological production as the likely cause for the majority of the $pCO_{2sw}$ change. This is consistent with the results of *Tremblay et al.* [2011] who calculated new phytoplankton production at high rates in Franklin Bay (48 gC m$^{-2}$ between mid-May and late June, or ~6 times the rate observed in 2004), and *Mundy et al.* [2009] who calculated similar production rates in Darnley Bay.

[22] Transects conducted the following week (Figure 5b) showed a very different pattern; we observed patches of $pCO_{2sw}$ up to 456 $\mu$atm, with the highest values just offshore of Cape Parry. The June 6 transect from Cape Parry to the Darnley Bay ice edge is detailed in Figure 6, and it reveals patterns of $pCO_{2sw}$ and salinity that indicate upwelling of high-salinity, $CO_2$-rich water. Particularly high $pCO_{2sw}$ was observed after occupying a station just inside the Darnley Bay ice edge on June 6 (Figure 7), in association with upwelling that was described in detail by *Mundy et al.* [2009]. From its peak on June 7, $pCO_{2sw}$ decreased to ~300 $\mu$atm along with salinity as PML water returned while the upwelling-favorable winds relaxed. *Mundy et al.* [2009] also detected a near-surface phytoplankton bloom triggered by this upwelling, which persisted for several days even though the nutrient maximum quickly retreated to below the surface. The continued decrease in $pCO_{2sw}$ evident in Figure 7 was likely a result of that bloom.

[23] After the upwelling, strongly negative $\Delta pCO_2$ was prevalent across the region for the rest of June (Figures 5c–5f). We measured $pCO_{2sw}$ minima of 232 $\mu$atm on June 18 in Darnley Bay, 212 $\mu$atm on June 23 in Franklin Bay, and 226 $\mu$atm on June 26 near Cape Parry. This continued reduction in $pCO_{2sw}$ no doubt reflected the strong biological productivity that continued through the month [*Tremblay et al.*, 2011; *Mundy et al.*, 2009], but sea ice melt likely played a significant role as well. For example, Figure 8 shows $pCO_{2sw}$ in relation to salinity and SST during the June 23 transect in Franklin Bay (Figure 5d). On this transect, the ship left a station near Cape Parry and navigated around a large floe of formerly landfast ice that had recently fractured and was drifting northwest. Near the southeastern edge of the floe, we encountered a patch of water that was fresher (by 8 units) and had lower $pCO_{2sw}$ (by 100 $\mu$atm) than water near Cape Parry or towards Cape Bathurst. Given the location of this patch at the trailing edge of the drifting floe, the low salinity must have been caused by ice melt. Measurements in Franklin and Darnley Bays revealed very low $pCO_2$ (0–188 $\mu$atm) in the brine of decaying ice [*Geilfus et al.*, 2012], confirming the link between low salinity and low $pCO_2$. The effect of ice melt associated with this particular drifting ice floe was also captured in two transects towards Cape Bathurst. On June 24 (before the floe drifted across the region), the transect yielded a constant $pCO_{2sw}$ of ~335 $\mu$atm (Figure 5d) and salinity of ~31, whereas the transect following the floe on June 27 (Figures 5f) revealed lower "ambient" $pCO_{2sw}$ (315 $\mu$atm) and
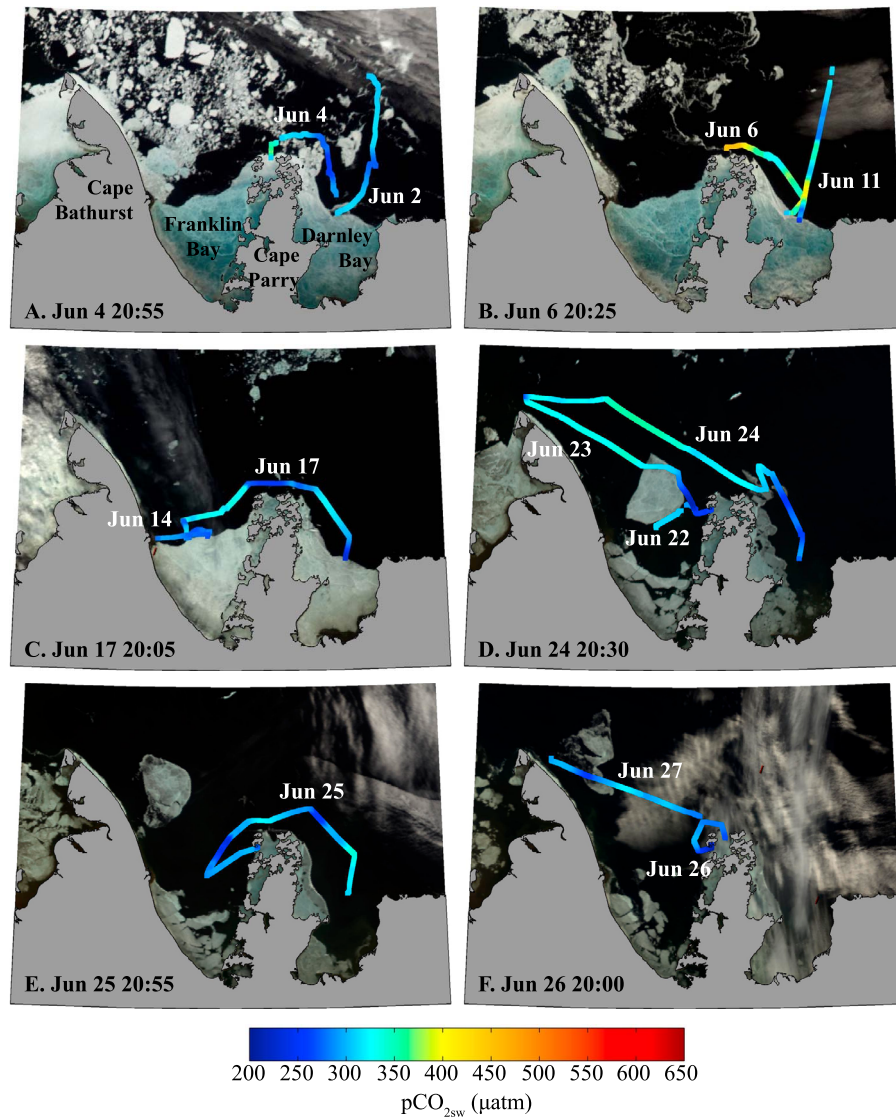
**Figure 5.** Measured $p$CO$_{2sw}$ ($\mu$atm) during transects conducted in June 2008. Transects are overlain on true-color MODIS imagery from the dates and times indicated.
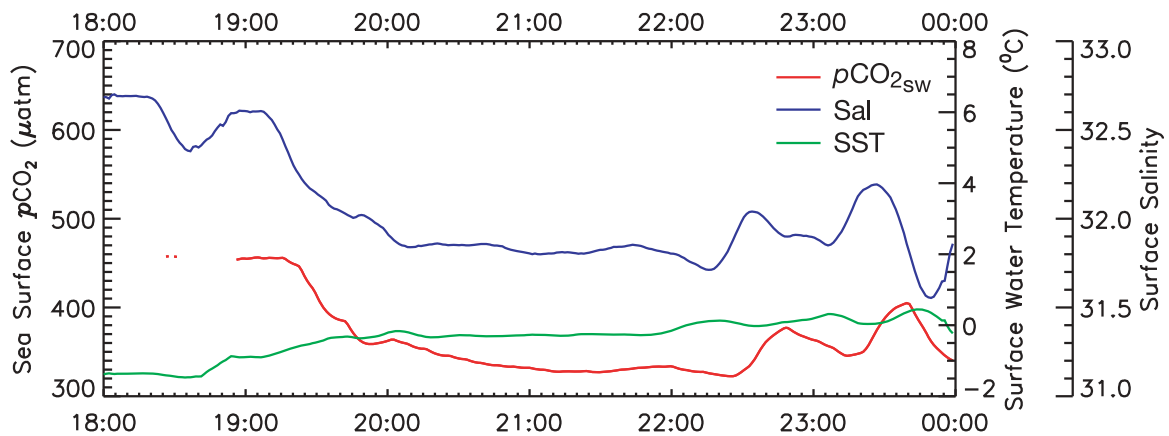


**Figure 6.** Measured $p$CO$_{2sw}$ ($\mu$atm, red line), surface salinity (blue line) and sea surface temperature (green line) during the June 6 transect from Cape Parry to Darnley Bay (Figure 5b). High salinity is associated with high $p$CO$_{2sw}$, indicating the influence of upwelling.
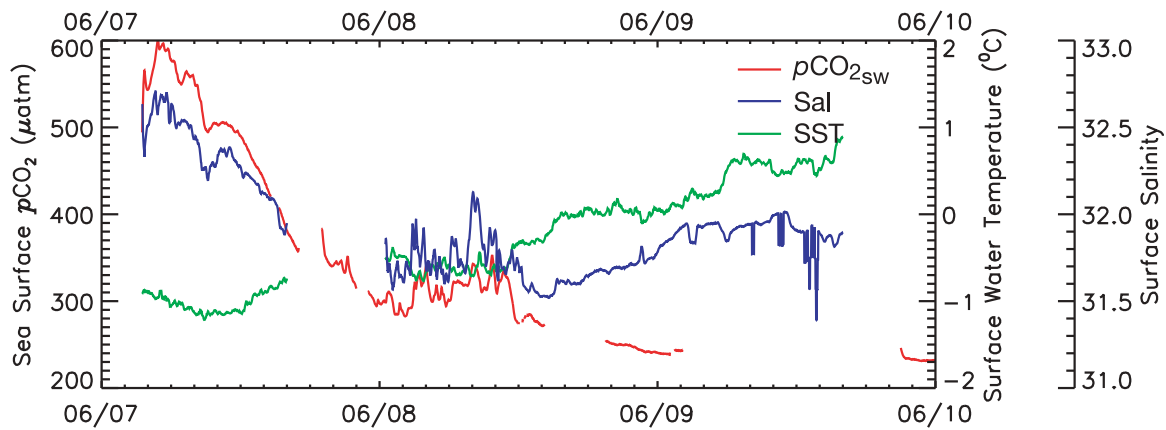
**Figure 7.** Measured $pCO_{2sw}$ ($\mu$atm, red line), surface salinity (blue line) and sea surface temperature (green line) at the Darnley Bay landfast ice edge station (Figure 5b) occupied from June 7–10. Initial high salinity and high $pCO_{2sw}$ were the result of upwelling.

salinity (29.5) with patches of $pCO_{2sw}$ as low as 240 $\mu$atm and associated low salinity (27.5). These results show that the breakup and decay of landfast ice affected $pCO_{2sw}$ over a large spatial domain.

### 3.2.  CO$_2$ Fluxes

#### 3.2.1.  Franklin Bay

[24] Estimated CO$_2$ fluxes across the air-sea interface in Franklin Bay are shown in Table 1, along with the key parameters used in the flux calculation. During the ship's initial visit to Franklin Bay (October 28), $\Delta pCO_2$ was $-20$ $\mu$atm, and we calculated an uptake of atmospheric CO$_2$ that was dampened by the high ($9/10^{ths}$) ice concentration. On our subsequent fall trips to the region $\Delta pCO_2$ had become significantly positive, and we calculated a strong outgassing (46 mmol m$^{-2}$ d$^{-1}$) on November 17 associated with a significant reduction in ice concentration (to $5/10^{ths}$, see Figure 2d). The switch from weak uptake to strong outgassing confounds whether Franklin Bay acted as a net source or sink of CO$_2$ during the fall. From October 30–November 12 there were strong easterly winds (Figure 3a), which means that upwelling may have resulted in

positive $\Delta pCO_2$ well before the ship returned to the area in mid-November. Hence, outgassing likely dominated towards the end of the freeze-up season, and Franklin Bay was probably a source of CO$_2$ to the atmosphere until exchange was limited by the formation of landfast ice.

[25] The flux calculations for the May trip to Franklin Bay are shown in Table 1 for the portion of the bay that had fractured in mid-April (section 3.1.2, Figure 4). Our calculations show outgassing of CO$_2$ at this time, but at very low rates ($<0.5$ mmol m$^{-2}$ d$^{-1}$) due to the high ice concentrations. When ice was finally exported out of the northern portion of the bay in June (Figure 5), we calculated fairly strong (mean values of $-3$–$-26$ mmol m$^{-2}$ d$^{-1}$) CO$_2$ uptake as $\Delta pCO_2$ became negative due to biological production and ice melt (Table 1). The eventual loss of ice from the southern portions of Franklin Bay (Figures 5e and 5f) allowed this uptake to occur over a large spatial extent, and the observed decrease in $pCO_{2sw}$ through the month of June suggests that uptake likely persisted beyond the end of our study (June 25). It therefore seems likely that Franklin Bay acted as a fairly
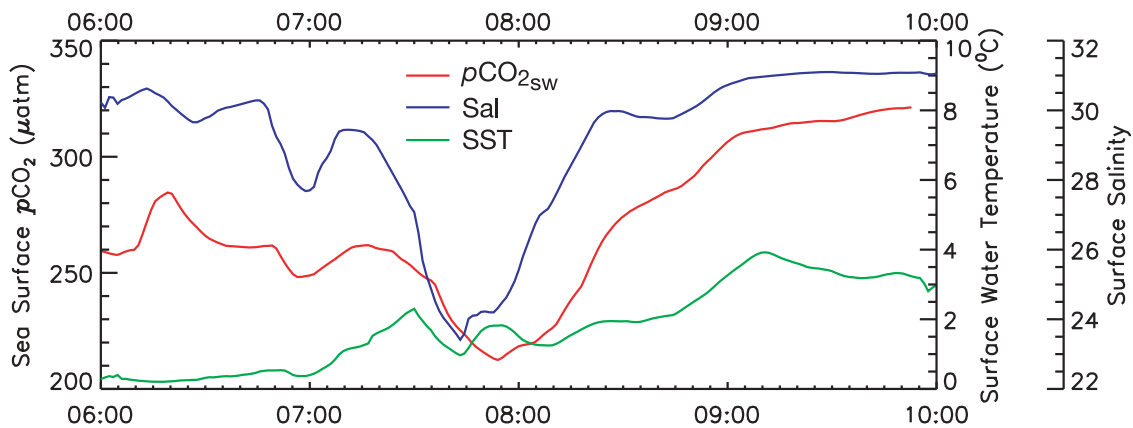


**Figure 8.** Measured $pCO_{2sw}$ ($\mu$atm, red line), surface salinity (blue line) and sea surface temperature (green line) during the June 23 transit around the decaying ice floe in Franklin Bay (Figure 5d). Low salinity is associated with low $pCO_{2sw}$, indicating the influence of ice melt.

**Table 1.** $CO_2$ Flux Estimates and Associated Parameters for the Franklin Bay Region[a]

| Date | Mean $pCO_{2sw}$ ($\mu$atm) | stddev $pCO_{2sw}$ ($\mu$atm) | $pCO_{2atm}$ ($\mu$atm) | $\Delta pCO_2$ ($\mu$atm) | $U$ (m/s) | $C_i$ (/10$^{ths}$) | $F_{CO_2}$ (mmol/m$^2$d) |
|---|---|---|---|---|---|---|---|
| Oct 28 | 363 | 9 | 383 | −22 | 6.9 | 9 | −0.4 |
| Nov 15 | 549 | 10 | 384 | 165 | | 9.7 | |
| Nov 17 | 510 | 8 | 389 | 121 | 15 | 5 | **46** |
| May 11–18 | 486 | 17 | 400 | 86 | 6 | 9.7 | **0.32** |
| Jun 14–18 | 287 | 14 | 390 | −103 | 3.0 | 0 | **−03.2** |
| Jun 20–22 | 301 | 10 | 391 | −90 | 7.4 | 0 | **−15.9** |
| Jun 25 | 287 | 12 | 393 | −106 | 8 | 0 | **−15.7** |
| Jun 26 | 253 | 21 | 391 | −138 | 8.7 | 0 | **−26.0** |

[a]Data were obtained on transects and station occupations depicted in Figures 2, 4 and 5.

strong sink of atmospheric $CO_2$ through the spring and early summer periods.

### 3.2.2. Darnley Bay

[26] On our first trip to Darnley Bay (November 6–11), we measured strongly positive $\Delta pCO_2$ (Table 2), similar to the November measurements in Franklin Bay. However, due to the complete landfast ice cover that existed at that time, we estimate that no outgassing from the seawater occurred. A subsequent storm created limited open water between November 7–18 in the northern half of Darnley Bay (Figure 2d) which may have allowed some outgassing, but the generally higher ice concentration probably resulted in less total outgassing than in Franklin Bay.

[27] In spring, Darnley Bay remained completely landfast until late June. For the most part, this prevented $CO_2$ exchange with the atmosphere, including potential outgassing associated with the early-June upwelling event (Figure 7). The ice finally broke up in Darnley Bay around June 21, permitting fluxes of $CO_2$ that reached $\sim$−22 mmol m$^{-2}$ d$^{-1}$ (Table 2). Hence, Darnley Bay likely acted as a sink of atmospheric $CO_2$ through the spring and early summer, similar to Franklin Bay.

### 3.2.3. Cape Parry and Cape Bathurst

[28] Tables 3 and 4 show that Cape Parry and Cape Bathurst also behaved in a similar fashion. We calculated modest outgassing ($\sim$1 mmol m$^{-2}$ d$^{-1}$) near the end of October in the Cape Bathurst region, followed by increasing ice concentration at both locations that would have limited further exchange. This shut-off was more dramatic at Cape Parry, where ice became landfast earlier and remained fast until the end of June. Ice stayed more mobile near Cape Bathurst, which would have allowed a more significant outgassing to occur through the fall until the ice became landfast in late December.

[29] In May, the landfast ice around Cape Parry prevented a potentially strong outgassing driven by the high ($\sim$125 $\mu$atm) $\Delta pCO_2$. No $pCO_{2sw}$ measurements were made in May in the Cape Bathurst region and therefore no flux calculations are available, but it is clear from Figure 4 that the area was covered

by very high concentrations of landfast ice, and was probably not involved in significant air-sea gas exchange.

[30] At Cape Bathurst the landfast ice began to break up in early June, and was completely exported by mid month. We calculated a weak $CO_2$ uptake in late June due to low wind velocities (Table 4), but we expect that the ice free conditions would have allowed significant uptake through the month. At Cape Parry $\Delta pCO_2$ was strongly negative through June, but the ice remained landfast, resulting in no calculated $CO_2$ uptake for the entire month. According to CIS charts the ice broke up in the first week of July, which likely would have permitted significant $CO_2$ uptake given the strongly negative $\Delta pCO_2$ observed at the end of June (Table 3). For both the Cape Bathurst and Cape Parry regions it is likely that significant uptake occurred through the rest of the open water season.

## 4. Discussion

### 4.1. Annual Air-Sea $CO_2$ Budgets

[31] Without a more complete time series of $pCO_{2sw}$ measurements and flux calculations, it is not possible to precisely assign an annual budget of air-sea $CO_2$ exchange to any of the landfast ice regions examined in this study. Nevertheless, it appears that the magnitude of outgassing during periods of $pCO_{2sw}$ supersaturation was limited by the presence of sea ice, whereas uptake was able to proceed freely once landfast ice was broken up and exported out of the study region. This seasonal cycle would result in a net annual uptake of $CO_2$, and is very similar to the "seasonal rectification" cycle described by *Yager et al.* [1995] for the Northeast Water polynya.

[32] A key aspect of this cycle in landfast ice regions is the assumed lack of air-sea gas exchange in winter due to the lack of open water. In offshore Amundsen Gulf, we observed episodes of $CO_2$ exchange 1–2 orders of magnitude higher than predicted by the bulk flux approach through open water associated with rapidly re-freezing leads [*Else et al.*, 2011].

**Table 2.** $CO_2$ Flux Estimates and Associated Parameters for the Darnley Bay Region[a]

| Date | Mean $pCO_{2sw}$ ($\mu$atm) | stddev $pCO_{2sw}$ ($\mu$atm) | $pCO_{2atm}$ ($\mu$atm) | $\Delta pCO_2$ ($\mu$atm) | $U$ (m/s) | $C_i$ (/10$^{ths}$) | $F_{CO_2}$ (mmol/m$^2$d) |
|---|---|---|---|---|---|---|---|
| Nov 6 | 530 | 14 | 390 | 140 | 5.6 | 10 | **0.0** |
| Nov 11 | 570 | 10 | | | | 10 | |
| Jun 2–4 | 293 | 10 | 392 | −99 | 5.2 | 10 | **0.0** |
| Jun 7–10 | 388 | 98 | 395 | −7 | 5.4 | 10 | **0.0** |
| Jun 11–14 | 243 | 12 | 390 | −147 | 1.5 | 10 | **0.0** |
| Jun 18–19 | 383 | 23 | 393 | −10 | 4.2 | 10 | **0.0** |
| Jun 24–25 | 303 | 13 | 396 | −93 | 10.6 | 2 | **−21.7** |
| Jun 27 | 313 | 14 | 392 | −79 | 3.9 | 0 | **−2.9** |

[a]Data were obtained on transects and station occupations depicted in Figures 2 and 5.

**Table 3.** $CO_2$ Flux Estimates and Associated Parameters for the Cape Parry Region[a]

| Date | Mean $pCO_{2sw}$ ($\mu$atm) | stddev $pCO_{2sw}$ ($\mu$atm) | $pCO_{2atm}$ ($\mu$atm) | $\Delta pCO_2$ ($\mu$atm) | $U$ (m/s) | $C_i$ (/10[ths]) | $F_{CO_2}$ (mmol/m²d) |
|---|---|---|---|---|---|---|---|
| Oct 28 | 508 | 4 | 384 | 124 | | 9.7 | |
| Nov 13 | 598 | 5 | 375 | 223 | | 10 | |
| Nov 18 | 575 | 3 | 384 | 191 | 12.7 | 10 | 0.0 |
| May 8 | 525 | 4 | 403 | 122 | | 10 | 0.0 |
| May 10 | 555 | 13 | 408 | 147 | 1.9 | 10 | 0.0 |
| Jun 4–6 | 445 | 38 | 394 | 51 | | 10 | 0.0 |
| Jun 22–23 | 270 | 7 | 390 | −20 | 0.9 | 10 | 0.0 |

[a]Data were obtained on transects and station occupations depicted in Figures 2, 4 and 5.

In *Else et al.* [2012], we argued that the seasonal rectification hypothesis does not hold in Amundsen Gulf because the frequent leads that occur in the area may permit significant air-sea gas exchange. This study shows that the seasonal rectification hypothesis is more applicable in the nearby landfast ice regions, where the lack of leads likely prevents winter outgassing.

[33] One exception to this generalized observation is the brief period of time in mid-November when the landfast ice in Franklin and Darnley Bays was mobilized by strong winds (Figures 2c and 2d), resulting in the high $CO_2$ outgassing we calculated in Franklin Bay on November 17 (Table 1). This event probably generated conditions very similar to the leads we observed in offshore Amundsen Gulf, and therefore the outgassing may have been even stronger than we calculated. Since this event was fairly short lived (less than 10 days) it probably does not compromise our conclusion that the regions acted as a net $CO_2$ sink in 2007–08, but it does suggest that the net annual exchange may be vulnerable to changes in winter ice conditions.

### 4.2. Upwelling Events in 2007–08

[34] A review of past studies conducted in landfast ice regions show that our observations of highly positive $\Delta pCO_2$ episodes are unique; persistently negative $\Delta pCO_2$ has been observed under landfast ice in Antarctica [*Gibson and Trull*, 1999] and Greenland [*Sejr et al.*, 2011], *Miller et al.* [2011] observed no supersaturation during the 2003–04 CASES overwintering project in Franklin Bay, and *Semiletov et al.* [2007] observed only modest supersaturation under landfast ice near Point Barrow, Alaska. The key difference for the landfast ice of southern Amundsen Gulf in 2007–08 therefore appears to be the fall/spring upwelling, which raises the question of whether such events are typical for the region.

[35] The first requirement for upwelling in this region is strong easterly winds. In comparison to the long-term (1979–2009) records, wind speeds recorded at the Cape Parry weather station were approximately 35% stronger than average in the fall of 2007, and 25% stronger than average in the spring of 2008. Furthermore, the mean easterly component of wind velocity was about 5 times stronger than average in the fall, and nearly 2 times stronger in the spring. As Figure 9 shows,

these strong easterlies were driven by a very steep pressure gradient caused by anomalously high pressure to the north of the study area and low pressure to the south. This structure is part of the "Arctic Dipole" pattern, which is strongly correlated with increasing fall open water in the western sector of the Arctic Ocean [*Overland and Wang*, 2010], a dominant feature in 2007 [*Perovich et al.*, 2008] and 2008 [*Maslanik et al.*, 2011].

[36] The second requirement for upwelling is an appropriate coastline or ice edge geometry. The area around Cape Bathurst is a well known site of significant upwelling in the presence of easterly winds [*Williams and Carmack*, 2008; *Mucci et al.*, 2010; *Tremblay et al.*, 2011] and Figure 2a shows that Cape Parry may act in a similar manner. In contrast, significant fall upwelling did not occur in Franklin Bay (Figure 2a) until an ice edge was established (Figures 2b–2d), despite upwelling-favorable winds earlier in the season (Figure 3a). Similarly, *Mundy et al.* [2009] hypothesized that the presence of an ice edge was necessary to force the early June upwelling event in Darnley Bay (Figure 5b). Although the spring breakup of landfast ice edges in 2008 was fairly typical for the region, they first formed in the fall around November 6, a condition that only occurs in about 25% of years [*Galley et al.*, 2008]. This suggests that there may have been a unique combination of strong winds and ice conditions that made the fall of 2007 particularly conducive to upwelling.

[37] If the upwelling in this region is indeed controlled by wind and ice conditions, then the air-sea $CO_2$ exchange cycle that we observed could be subject to significant interannual variability. For example, in years where upwelling does not occur (as appeared to be the case in 2004 [*Miller et al.*, 2011; *Tremblay et al.*, 2011]), the presence or absence of landfast ice in the fall and spring may not be important in preventing outgassing and maintaining a net annual sink. However, given observations of the Arctic Dipole pattern beginning to dominate circulation in the Arctic [*Overland and Wang*, 2010; *Maslanik et al.*, 2007, 2011], upwelling favorable winds may become more common in this region. If that is the case, the maintenance of a net atmospheric $CO_2$ sink may lie with the fate of the landfast ice. Presently, no trends in landfast ice duration, breakup date, or freeze-up date have

**Table 4.** $CO_2$ Flux Estimates and Associated Parameters for the Cape Bathurst Region[a]

| Date | Mean $pCO_{2sw}$ ($\mu$atm) | stddev $pCO_{2sw}$ ($\mu$atm) | $pCO_{2atm}$ ($\mu$atm) | $\Delta pCO_2$ ($\mu$atm) | $U$ (m/s) | $C_i$ (/10[ths]) | $F_{CO_2}$ (mmol/m²d) |
|---|---|---|---|---|---|---|---|
| Oct 29 | 493 | 25 | 385 | 108 | 9.0 | 9.7 | 0.8 |
| Oct 30 | 557 | 14 | 385 | 172 | 9.8 | 9.7 | 1.2 |
| Jun 23–24 | 324 | 4 | 391 | −67 | 5.5 | 0 | −4.9 |

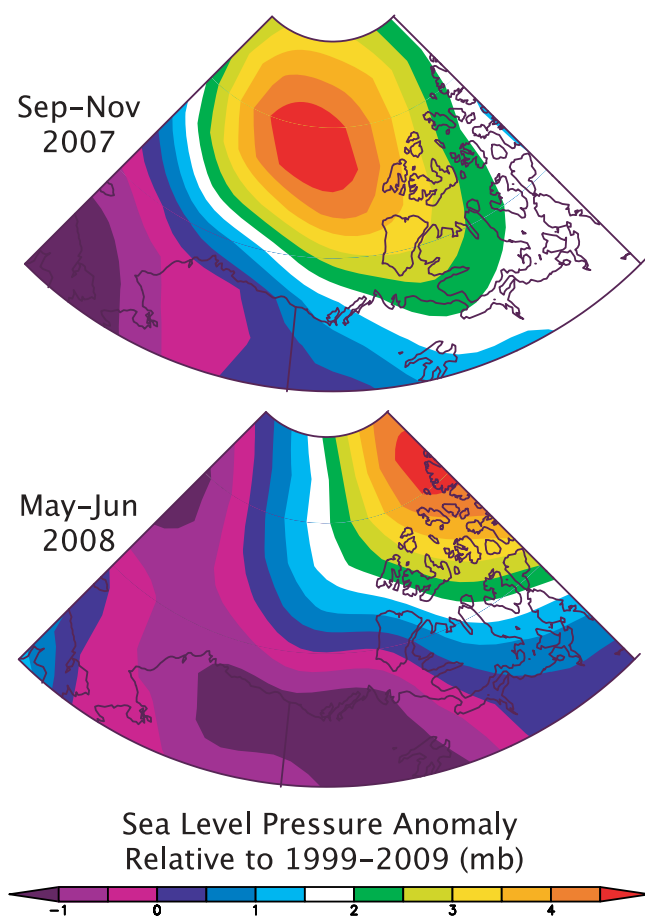[a]Data were obtained on transects and station occupations depicted in Figures 2 and 5.

**Figure 9.** Seasonal pressure anomalies relative to the decadal (1999–2009) mean. Data are from the NCEP/NARR reanalysis [*Kalnay et al.*, 1996], plotted using the web-based plotting tools of the NOAA/ESRL Physical Sciences Division (Boulder, Colorado).

been identified for this region, but other areas of the Canadian Arctic are showing signs of a transition to a shorter landfast ice season [*Galley et al.*, 2012]. Since strong upwelling events in the absence of sea ice do have the potential to switch a region from net annual uptake to net annual outgassing [*Mathis et al.*, 2012], a shorter landfast ice season in conjunction with increased upwelling (keeping in mind that upwelling at the Capes can occur without a landfast ice edge), could break down the net annual atmospheric $CO_2$ sink that we have proposed for this region.

## 5. Conclusions

[38] The landfast ice regions of southern Amundsen Gulf likely acted as net annual sinks for atmospheric $CO_2$ in 2007–08. Upwelling episodes generated positive $\Delta pCO_2$ in late fall and early spring, but we calculated that high ice concentrations prevented significant outgassing. In contrast, primary production and ice melt caused negative $\Delta pCO_2$ in late spring and early summer, which allowed significant $CO_2$ uptake once the landfast ice broke up and was exported. This cycle of inhibited outgassing in the fall/spring and free uptake in the summer is similar to the cycle proposed by *Yager et al.* [1995] for Arctic polynya regions, but is different from other

recent observations in landfast ice regions [*Gibson and Trull*, 1999; *Miller et al.*, 2011; *Sejr et al.*, 2011]. The main difference in our study was the occurrence of upwelling events, caused by abnormally strong easterly winds. In some areas, the presence or absence of a landfast ice edge seemed to be an additional requirement for strong upwelling. The importance of these two variables (easterly winds and ice edge position) to our observations suggests that air-sea $CO_2$ exchange in the region may be subject to significant interannual variability. It also suggests a vulnerability to climate change, particularly if observed changes in Arctic atmospheric circulation [e.g., *Maslanik et al.*, 2007; *Overland and Wang*, 2010] and landfast ice conditions [e.g., *Galley et al.*, 2012] continue on their current trajectory.

## References

ArcticNet Inc. (2010), *Impacts of Environmental Change in the Canadian Coastal Arctic: A Compendium of Research Conducted During ArcticNet Phase I (2004–2008)*, Quebec City, Quebec, Canada.

Barber, D. G., M. G. Aplin, Y. Gratton, J. V. Lukovich, R. J. Galley, R. L. Raddatz, and D. Leitch (2010), The International Polar Year (IPY) Circumpolar Flaw Lead (CFL) system study: Overview and the physical system, *Atmos. Ocean*, 48(4), 225–243, doi:10.3137/OC317.2010.

Dieckmann, G. S., G. Nehrke, S. Papadimitriou, J. Göttlicher, R. Steininger, H. Kennedy, D. Wolf-Gladrow, and D. N. Thomas (2008), Calcium carbonate as ikaite crystals in Antarctic sea ice, *Geophys. Res. Lett.*, 35, L08501, doi:10.1029/2008GL033540.

Else, B. G. T., T. N. Papakyriakou, R. J. Galley, W. M. Drennan, L. A. Miller, and H. Thomas (2011), Wintertime $CO_2$ fluxes in an Arctic polynya using eddy covariance: Evidence for enhanced air-sea gas transfer during ice formation, *J. Geophys. Res.*, 116, C00G03, doi:10.1029/2010JC006760.

Else, B. G. T., T. N. Papakyriakou, R. J. Galley, A. Mucci, M. Gosselin, L. A. Miller, E. H. Shadwick, and H. Thomas (2012), Annual cycles of $pCO_{2sw}$ in the southeastern Beaufort Sea: New understandings of air-sea $CO_2$ exchange in arctic polynya regions, *J. Geophys. Res.*, 117, C00G13, doi:10.1029/2011JC007346.

Fransson, A., M. Chierici, and Y. Nojiri (2009), New insights into the spatial variability of the surface water carbon dioxide in varying sea ice conditions in the Arctic Ocean, *Cont. Shelf Res.* 29(10), 1317–1328, doi:10.1016/j.csr.2009.03.008.

Galley, R. J., E. Key, D. G. Barber, B. J. Hwang, and J. K. Ehn (2008), Spatial and temporal variability of sea ice in the southern Beaufort Sea and Amundsen Gulf: 1980–2004, *J. Geophys. Res.*, 113(C5), C05S95, doi:10.1029/2007JC004553.

Galley, R. J., B. G. T. Else, J. V. Lukovich, S. E. L. Howell, and D. G. Barber (2012), Landfast sea ice conditions in the Canadian Arctic: 1983–2009, *Arctic*, 65(2), 133–144.

Geilfus, N.-X., G. Carnat, T. Papakyriakou, J.-L. Tison, B. Else, H. Thomas, E. Shadwick, and B. Delille (2012), Dynamics of $pCO_2$ and related air-ice $CO_2$ fluxes in the Arctic coastal zone (Amundsen Gulf, Beaufort Sea), *J. Geophys. Res.*, 117, C00G10, doi:10.1029/2011JC007118.

Gibson, J. A. E., and T. W. Trull (1999), Annual cycle of $f$CO$_2$ under sea-ice and in open water in Prydz Bay, East Antarctica, *Mar. Chem.*, *66*, 187–200, doi:10.1016/S0304-4203(99)00040-7.

Gosink, T. A., J. G. Pearson, and J. J. Kelley (1976), Gas movement through sea ice, *Nature*, *263*, 41–42.

Jacobs, J. D., R. G. Barry, and R. L. Weaver (1975), Fast ice characteristics, with special reference to the eastern Canadian Arctic, *Polar Rec.*, *17*, 521–536, doi:10.1017/S0032247400032484.

Jähne, B., G. Heinz, and W. Dietrich (1987), Measurement of the diffusion coefficients of sparingly soluble gases in water, *J. Geophys. Res.*, *92*(C10), 10,767–10,776, doi:10.1029/JC092iC10p10767.

Kalnay, E., et al. (1996), The NCEP/NCAR 40-year reanalysis project, *Bull. Am. Meteorol. Soc.*, *77*, 437–471.

Lansard, B., A. Mucci, L. A. Miller, R. W. MacDonald, and Y. Gratton (2012), Seasonal variability of water mass distribution in the southeastern Beaufort Sea determined by total alkalinity and $\delta^{18}$O, *J. Geophys. Res.*, *117*, C03003, doi:10.1029/2011JC007299.

Loose, B., P. Schlosser, D. Perovich, D. Ringelberg, D. T. Ho, T. Takahashi, J. Richter-Menge, C. M. Reynolds, W. R. McGillis, and J.-L. Tison (2011), Gas diffusion through columnar laboratory sea ice: Implications for mixed-layer ventilation of CO$_2$ in the seasonal sea ice zone, *Tellus, Ser. B*, *63*, 23–39, doi:10.1111/j.1600-0889.2010.00506.x.

Maslanik, J., S. Drobot, C. Fowler, W. Emery, and R. Barry (2007), On the Arctic climate paradox and the continuing role of atmospheric circulation in affecting sea ice conditions, *Geophys. Res. Lett.*, *34*, L03711, doi:10.1029/2006GL028269.

Maslanik, J., J. Stroeve, C. Fowler, and W. Emery (2011), Distribution and trends in Arctic sea ice age through spring 2011, *Geophys. Res. Lett.*, *38*, L13502, doi:10.1029/2011GL047735.

Mathis, J. T., et al. (2012), Storm-induced upwelling of high $p$CO$_2$ waters onto the continental shelf of the western Arctic Ocean and implications for carbonate mineral saturation states, *Geophys. Res. Lett.*, *39*, L07606, doi:10.1029/2012GL051574.

Miller, L. A., et al. (2002), Carbon distributions and fluxes in the North Water, 1998 and 1999, *Deep Sea Res., Part II*, *49*, 5151–5170.

Miller, L. A., T. N. Papakyriakou, R. E. Collins, J. W. Deming, J. K. Ehn, R. W. Macdonald, A. Mucci, O. Owens, M. Raudsepp, and N. Sutherland (2011), Carbon dynamics in sea ice: A winter flux time series, *J. Geophys. Res.*, *116*, C02028, doi:10.1029/2009JC006058.

Mucci, A., B. Lansard, L. A. Miller, and T. N. Papakyriakou (2010), CO$_2$ fluxes across the air-sea interface in the southeastern Beaufort Sea: Ice-free period, *J. Geophys. Res.*, *115*, C04003, doi:10.1029/2009JC005330.

Mundy, C. J., et al. (2009), Contribution of under-ice primary production to an ice-edge upwelling phytoplankton bloom in the Canadian Beaufort Sea, *Geophys. Res. Lett.*, *36*, L17601 doi:10.1029/2009GL038837.

Nomura, D., H. Eicken, R. Gradinger, and K. Shirasawa (2010), Rapid physically driven inversion of the air-sea ice CO$_2$ flux in the seasonal landfast ice off Barrow, Alaska after onset of surface melt, *Cont. Shelf Res.*, *30*, 1998–2004, doi:10.1016/j.csr.2010.09.014.

Overland, J. E., and M. Wang (2010), Large-scale atmospheric circulation changes are associated with the recent loss of Arctic sea ice, *Tellus, Ser. A*, *62*, 1–9, doi:10.1111/j.1600-0870.2009.00421.x.

Papakyriakou, T., and L. Miller (2011), Springtime CO$_2$ exchange over seasonal sea ice in the Canadian Arctic Archipelago, *Ann. Glaciol.*, *52*(57), 215–224.

Perovich, D. K., J. A. Richter-Menge, K. F. Jones, and B. Light (2008), Sunlight, water and ice: Extreme Arctic sea ice melt during the summer of 2007, *Geophys. Res. Lett.*, *35*, L11501, doi:10.1029/2008GL034007.

Rysgaard, S., R. N. Glud, M. K. Sejr, J. Bendtsen, and P. B. Christensen (2007), Inorganic carbon transport during sea ice growth and decay: A carbon pump in polar seas, *J. Geophys. Res.*, *112*, C03016, doi:10.1029/2006JC003572.

Rysgaard, S., J. Bendtsen, L. T. Pedersen, H. Ramløv, and R. N. Glud (2009), Increased CO$_2$ uptake due to sea ice growth and decay in the Nordic Seas, *J. Geophys. Res.*, *114*, C09011, doi:10.1029/2008JC005088.

Sejr, M. K., D. Krause-Jensen, S. Rysgaard, L. L. Sørensen, P. B. Christensen, and R. N. Glud (2011), Air-sea flux of CO$_2$ in arctic coastal waters influenced by glacial melt water and sea ice, *Tellus, Ser. B*, *63*, 815–822, doi:10.1111/j.1600-0889.2011.00540.x.

Semiletov, I., A. Makshtas, S.-I. Akasofu, and E. L. Andreas (2004), Atmospheric CO$_2$ balance: The role of Arctic sea ice, *Geophys. Res. Lett.*, *31*, L05121, doi:10.1029/2003GL017996.

Semiletov, I. P., I. I. Pipko, I. Repina, and N. E. Shakhova (2007), Carbonate chemistry dynamics and carbon dioxide fluxes across the atmosphere–ice–water interfaces in the Arctic Ocean: Pacific sector of the Arctic, *J. Mar. Syst.*, *66*, 204–226, doi:10.1016/j.jmarsys.2006.05.012.

Shadwick, E. H., et al. (2011), Seasonal variability of the inorganic carbon system in the Amundsen Gulf region of the southeastern Beaufort Sea, *Limnol. Oceanogr.*, *56*(1), 303–322, doi:10.4319/lo.2011.56.1.0303.

Sweeney, C., E. Gloor, A. R. Jacobson, R. M. Key, G. McKinley, J. L. Sarmiento, and R. Wanninkhof (2007), Constraining global air-sea gas exchange for CO$_2$ with recent bomb $^{14}$C measurements, *Global Biogeochem. Cycles*, *21*, GB2015, doi:10.1029/2006GB002784.

Takahashi, T., J. Olafsson, J. G. Goddard, D. W. Chipman, and S. C. Sutherland (1993), Seasonal variation of CO$_2$ and nutrients in the high-latitude surface oceans: A comparative study, *Global Biogeochem. Cycles*, *7*(4), 843–878.

Tremblay, J.-É., et al. (2011), Climate forcing multiplies biological productivity in the coastal Arctic Ocean, *Geophys. Res. Lett.*, *38*, L18604, doi:10.1029/2011GL048825.

Weiss, W. J., and B. A. Price (1980), Nitrous oxide solubility in water and seawater, *Mar. Chem.*, *8*(4), 347–359, doi:10.1016/0304-4203(80)90024-9.

Williams, W. J., and E. C. Carmack (2008), Combined effect of wind-forcing and isobath divergence on upwelling at Cape Bathurst, Beaufort Sea, *J. Mar. Res.*, *66*(5), 645–663, doi:10.1357/002224008787536808.

Woolf, D. K. (2005), Parameterization of gas transfer velocities and sea-state-dependent wave breaking, *Tellus, Ser. B*, *57*, 87–94.

Yager, P. L., D. W. R. Wallace, K. M. Johnson, W. O. Smith Jr., P. J. Minnett, and J. W. Deming (1995), The Northeast Water Polynya as an atmospheric CO$_2$ sink: A seasonal rectification hypothesis, *J. Geophys. Res.*, *100*(C3), 4389–4398, doi:10.1029/94JC01962.